Supporting Information

Indenone-fused *N*-heteroacenes

Fangwei Ding,[a] Debin Xia,*[a] Congwu Ge,[b] Zhenchao Kang,[a] Yulin Yang,[a] Ruiqing Fan,[a] Kaifeng Lin*[a] and Xike Gao*[b]

[a] MIIT Key Laboratory of Critical Materials Technology for New Energy Conversion and Storage, School of Chemistry and Chemical Engineering, Harbin Institute of Technology, Harbin 150001, China

[b] Key Laboratory of Synthetic and Self-Assembly Chemistry for Organic Functional Molecules, Shanghai Institute of Organic Chemistry Chinese Academy of Sciences

*E-mail: xia@hit.edu.cn
linkaifeng@hit.edu.cn
gaoxk@mail.sioc.ac.cn

Table of Contents

1. General information

Unless otherwise noted, all reagents were obtained from commercial suppliers and were used without further purification. ^{1}H NMR (400 MHz or 500 MHz) and ^{13}C NMR (100 MHz) spectra were obtained on Bruker 400 M or 500 M nuclear resonance spectrometers. Chemical shifts are reported in ppm from tetramethylsilane with the solvent resonance as the internal standard. The following abbreviations were used to designate chemical shift multiplicities: s = singlet, d = doublet, t = triplet, m = multiplet. Flash column chromatography was performed using 200-300 mesh silica gel. To gain more insight into the frontier energy levels, density functional theory (DFT) calculation were performed on all the products using Gaussian 09 program with the 6-311++G** basis set. Cyclic voltammetry experiments were conducted in dichlormethane at room temperature using 0.1 M Bu_4NPF_6 as the electrolyte. TGA measurement was carried out under N_2 atmosphere, heating rate: 10 ^{o}C min^{-1}.

We used space-charge-limited current (SCLC) method with device configuration of glass/Al/active layer/Al and ITO/PEDPOT:PSS/active layer/Au to measure the electron and hole mobility, respectively. According to Mott – Gurney law, SCLC theory can be described by the equation (1), where J is the current density, ε_0 is the permittivity of vacuum, ε_r is the relative permittivity of the material, μ is the mobility, V_a is the applied voltage, V_{bi} is the built-in voltage, which results from the difference in the work function of the anode and the cathode, and d (70 nm) is the thickness of the active film.

$$J = \frac{9}{8}\varepsilon_0\varepsilon_r\mu\frac{(V_a - V_{bi})^2}{d^3} \quad (1)$$

The synthesis of **3a-3e**.

A solution of diamine **1a-1d** (0.1 mmol, 1.0 equiv) and **2a** or **2b** (0.12 mmol, 1.2 equiv) with 2 mL acetic acid was prepared in a round-bottom flask fitted with a condenser. The stirred solution was heated to 100 ^{o}C for 1 h. The mixture was cooled to room temperature and then concentrated under reduced pressure. Finally, the crude products were purified by column chromatography using petroleum ether/DCM to afford the corresponding products (**3a-3e**).

The photographs of target products (**3a-3e**)

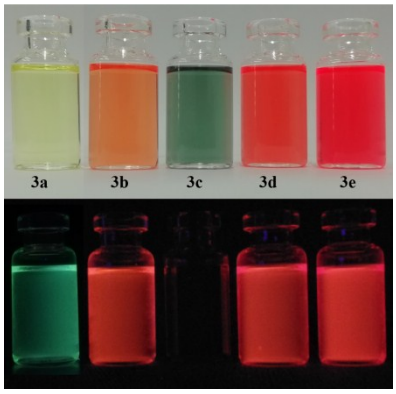

Figure S1**.** photographs of **3a-3e** in the daylight (top), and under 365nm UV (bottom) in CH_2Cl_2.

2. Experimental details

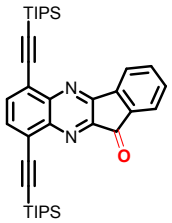

6,9-bis((triisopropylsilyl)ethynyl)-11H-indeno[1,2-b]quinoxalin-11-one (**3a)** The product was obtained as a red solid, m.p. 118-119 °C ^{1}H NMR (400 MHz, Chloroform-*d*) δ 8.06 (d, *J* = 7.5 Hz, 1H), 7.89 (dd, *J* = 9.1, 7.5 Hz, 2H), 7.84 – 7.72 (m, 2H), 7.61 (td, *J* = 7.5, 1.0 Hz, 1H), 1.25 (s, 21H), 1.23 (s, 21H). ^{13}C NMR (125 MHz, $CDCl_3$) δ 189.44, 157.28, 150.00, 143.98, 143.73, 141.49, 137.27, 136.77, 135.64, 133.48, 132.77, 126.37, 124.68, 124.39, 122.93, 103.07, 102.70, 102.33, 100.56, 18.97, 18.89, 11.61. IR (KBr): 2924, 2863, 2154, 1730, 1608, 1550, 1191, 1076, 883, 791, 674, 589 cm^{-1} MALDI-TOF MS, calculated for $C_{37}H_{48}N_2OSi_2$ $[M+H]^+$ 593.3, found 593.3 CCDC: 1951243

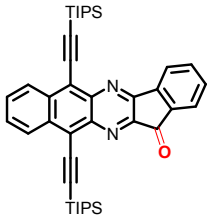

6,11-bis((triisopropylsilyl)ethynyl)-13H-benzo[g]indeno[1,2-b]quinoxalin-13-one (**3b)** The product was obtained as a red solid, m.p. 171-172 °C. ^{1}H NMR (400 MHz, Chloroform-*d*) δ 8.71 (ddd, *J* = 7.9, 4.5, 1.7 Hz, 2H), 8.17 (d, *J* = 7.6 Hz, 1H), 7.96 (d, *J* = 7.5 Hz, 1H), 7.81 (td, *J* = 7.5, 1.1 Hz, 1H), 7.73 (m, 2H), 7.68 – 7.62 (m, 1H), 1.31 (dd, *J* = 10.1, 3.8 Hz, 42H). ^{13}C NMR (100 MHz, $CDCl_3$) δ 189.12, 155.99, 151.02, 141.72, 141.07, 140.88, 138.48, 136.86, 135.68, 134.37, 133.00, 129.43, 128.49, 128.06, 127.70, 124.67, 124.48, 123.25, 121.40, 109.48, 107.11, 102.03, 101.55, 19.11, 19.01, 11.74, 11.72. IR (KBr): 2941, 2864, 2130, 1734, 1463, 1384, 1222, 1060, 881,758, 666, 469 cm^{-1} MALDI-TOF MS, calculated for $C_{41}H_{50}N_2OSi_2$ [m/z] 642.3, found 642.3 CCDC: 1951249

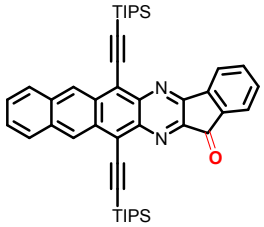

6,13-bis((triisopropylsilyl)ethynyl)-15H-indeno[1,2-b]naphtho[2,3-g]quinoxalin-15-one **(3c)** The product was obtained as a black solid, m.p. 204-205 °C. ^{1}H NMR (500 MHz, Chloroform-*d*) δ 9.37 (d, *J* = 18.7 Hz, 2H), 8.20 (d, *J* = 7.5 Hz, 1H), 8.12 – 8.03 (m, 2H), 7.99 (d, *J* = 7.5 Hz, 1H), 7.83 (td, *J* = 7.5, 1.1 Hz, 1H), 7.66 (t, *J* = 7.4 Hz, 1H), 7.56 (m, 2H), 1.37 (dd, *J* = 10.4, 4.4 Hz, 42H). ^{13}C NMR (125 MHz, $CDCl_3$) δ 188.80, 155.23, 151.29, 141.60, 140.60, 140.19, 138.99, 136.87, 133.72, 133.09, 133.07, 132.42, 131.55, 128.96, 128.79, 127.80, 127.49, 127.13, 127.12, 125.05, 124.62, 123.35, 121.40, 110.61, 107.98, 102.69, 102.21, 19.14, 19.06, 11.81, 11.79. IR (KBr): 2924, 2860, 2144, 1734, 1616, 1465, 1366, 1234, 1062, 1015, 882, 739, 671, 581, 463 cm^{-1} MALDI-TOF MS, calculated for $C_{45}H_{52}N_2OSi_2$ [m/z] 692.4, found 692.4 CCDC: 1951250

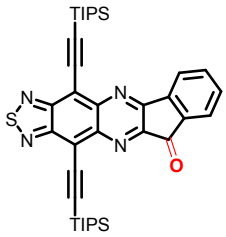

4,12-bis((triisopropylsilyl)ethynyl)-10H-indeno[1,2-b][1,2,5]thiadiazolo[3,4-g]quinoxalin-10-one **(3d)**

The product was obtained as a red solid, m.p. 168-169 °C. ^{1}H NMR (400 MHz, Chloroform-*d*) δ 8.20 (d, *J* = 7.5 Hz, 1H), 8.01 (d, *J* = 7.5 Hz, 1H), 7.86 (td, *J* = 7.5, 1.1 Hz, 1H), 7.71 (t, *J* = 7.5 Hz, 1H), 1.30 (dd, *J* = 10.0, 4.5 Hz, 42H). ^{13}C NMR (100 MHz, $CDCl_3$) δ 188.17, 156.06, 155.66, 154.62, 152.36, 143.09, 142.93, 141.23, 139.25, 137.19, 133.72, 124.86, 123.70, 118.37, 115.37, 112.95, 109.91, 100.65, 100.33, 19.04, 18.95, 11.70, 11.68. IR (KBr): 2941, 2864, 1737, 1623, 1462, 1361, 1237, 1157, 1073, 1018, 881, 677, 592 cm^{-1} MALDI-TOF MS, calculated for $C_{37}H_{46}N_4OSSi_2$ $[M+H]^+$ 651.3, found 651.3 CCDC: 1951263

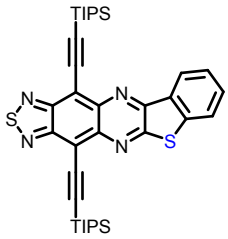

4,12-bis((triisopropylsilyl)ethynyl)benzo[4,5]thieno[2,3-b][1,2,5]thiadiazolo[3,4-g]quinoxaline **(3e)**

The product was obtained as a red solid, m.p. 218-219 °C. ^{1}H NMR (400 MHz, Chloroform-*d*) δ 8.55 (d, *J* = 7.7 Hz, 1H), 7.81 (d, *J* = 7.9 Hz, 1H), 7.67 (t, *J* = 7.6 Hz, 1H), 7.56 (t, *J* = 7.5 Hz, 1H), 1.31 (dd, *J* = 14.2, 4.5 Hz, 42H). ^{13}C NMR (100 MHz, $CDCl_3$) δ 160.50, 154.23, 154.13, 150.49, 141.79, 141.39, 141.18, 132.70, 130.91, 126.33, 125.62, 123.95, 114.99, 113.48, 110.06, 109.70, 101.33, 101.25, 19.09, 19.01, 11.75. IR (KBr): 2925, 2862, 1461, 1361, 1261, 1074, 1017, 881, 788, 678, 586 cm^{-1} MALDI-TOF MS, calculated for $C_{36}H_{46}N_4S_2Si_2$ [m/z] 654.3, found 654.3 CCDC: 1951264

3.The fluorescence spectroscopy

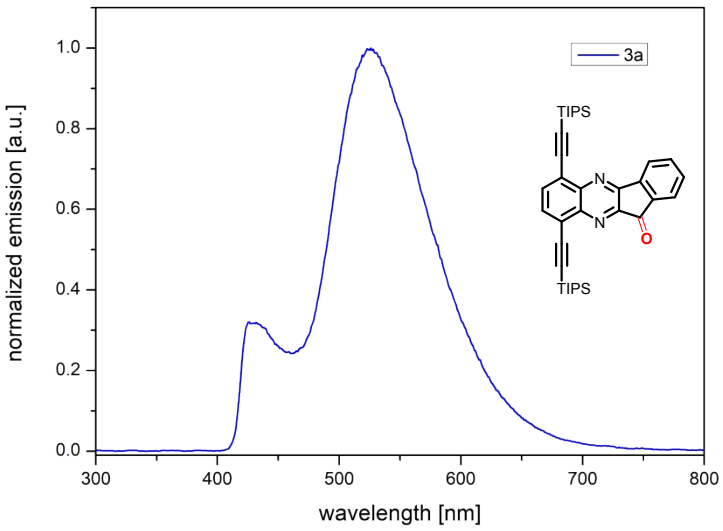

Figure S2. Fluorescence spectra of **3a** in CH_2Cl_2

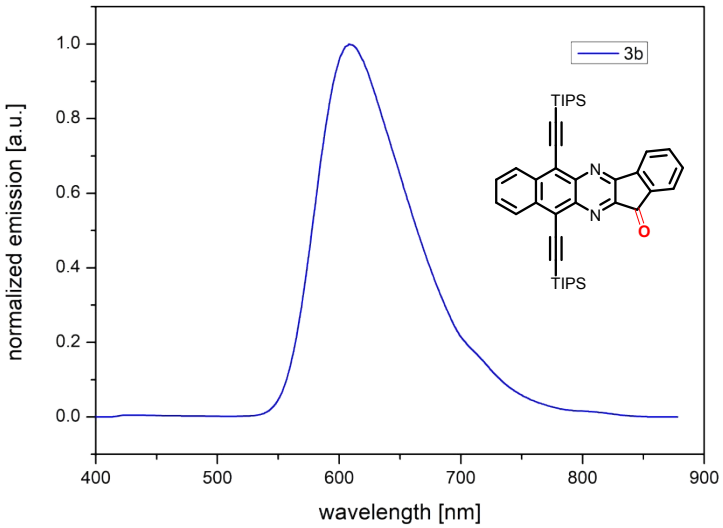

Figure S3. Fluorescence spectra of **3b** in CH_2Cl_2

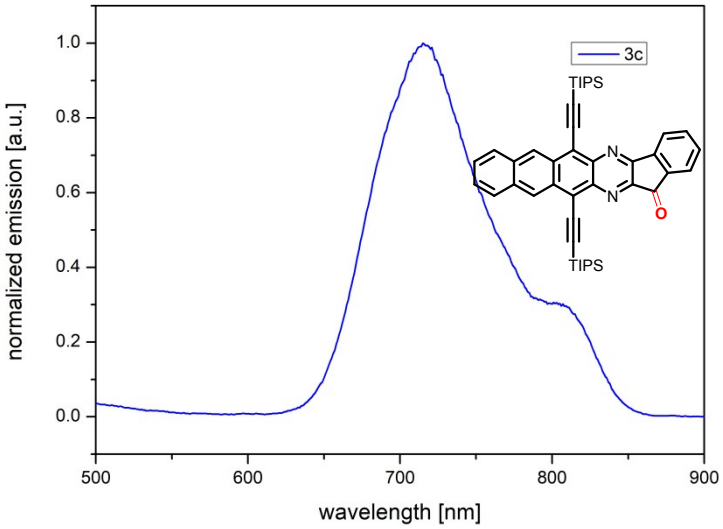

Figure S4. Fluorescence spectra of **3c** in CH_2Cl_2

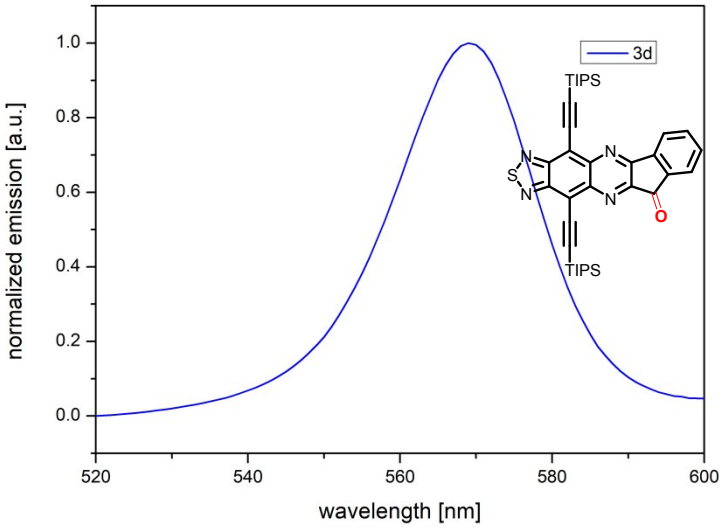

Figure S5. Fluorescence spectra of **3d** in CH_2Cl_2

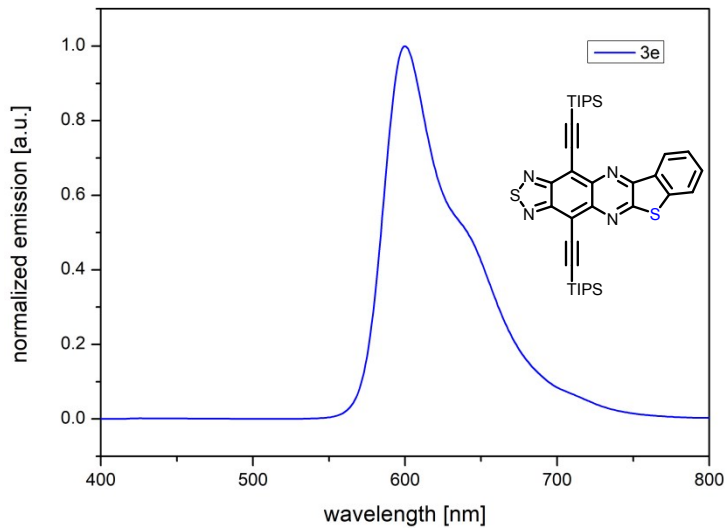

Figure S6. Fluorescence spectra of **3e** in CH_2Cl_2

4. The cyclic voltammetry and differential pulse voltammetry of target products

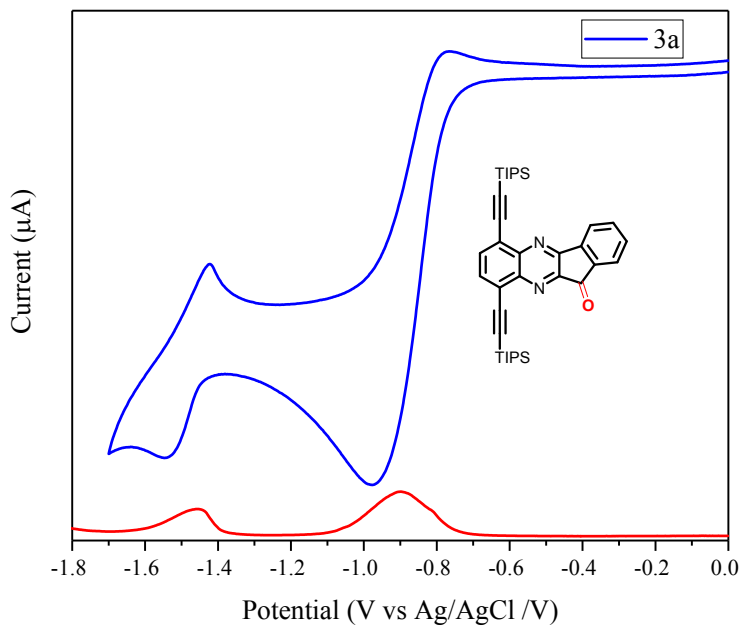

Figure S7. The DPV (red) and CV (blue) of **3a** in CH_2Cl_2 and 0.1 M Bu_4NPF_6 on a Pt electrode at a scan rate of 50 mVs^{-1} vs Ag/AgCl wire.

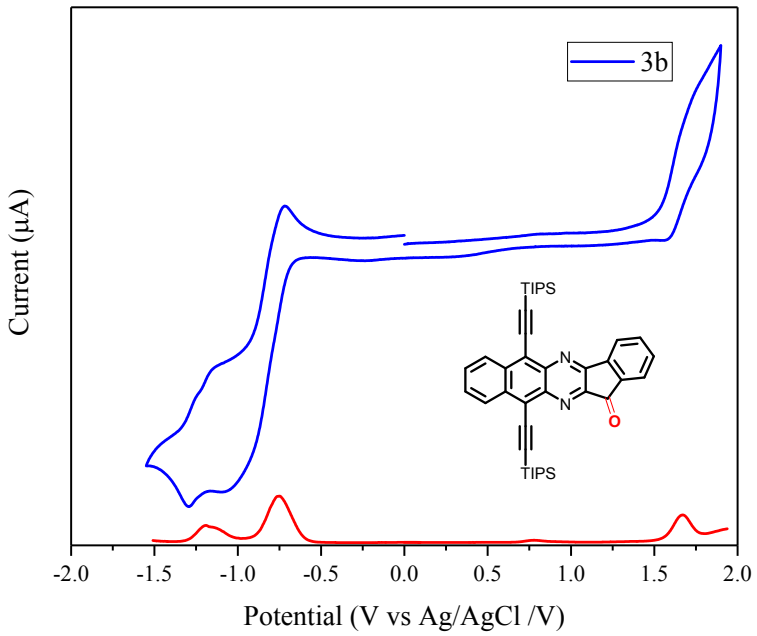

Figure S8. The DPV (red) and CV (blue) of **3b** in CH_2Cl_2 and 0.1 M Bu_4NPF_6 on a Pt electrode at a scan rate of 50 mVs^{-1} vs Ag/AgCl wire.

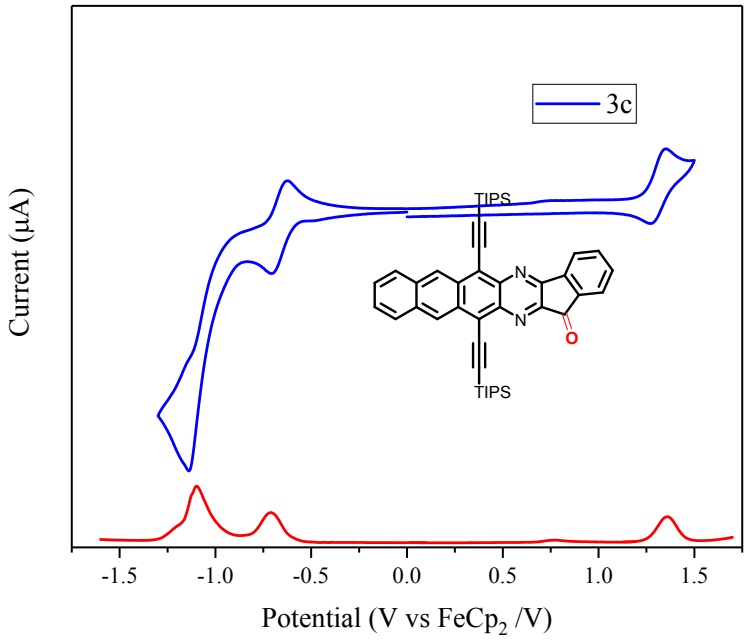

Figure S9. The DPV (red) and CV (blue) of **3c** in CH_2Cl_2 and 0.1 M Bu_4NPF_6 on a Pt electrode at a scan rate of 50 mVs^{-1} vs Ag/AgCl wire.

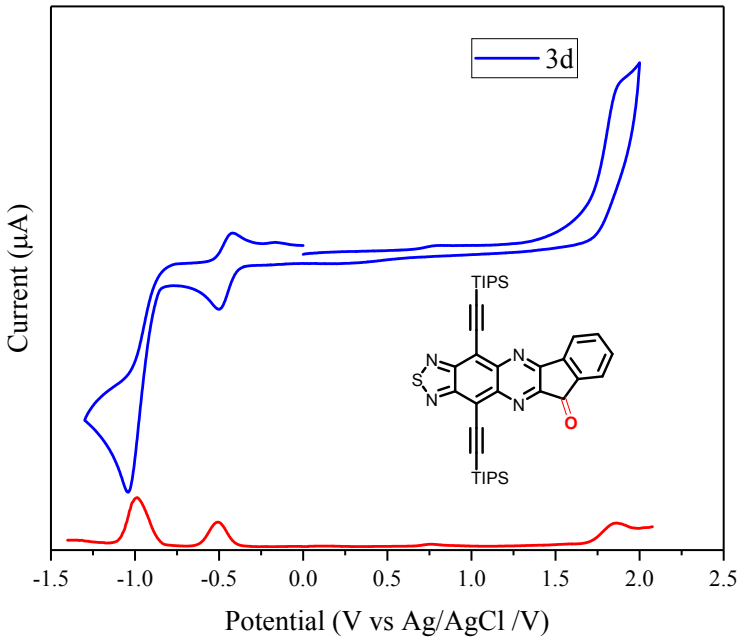

Figure S10. The DPV (red) and CV (blue) of **3d** in CH_2Cl_2 and 0.1 M Bu_4NPF_6 on a Pt electrode at a scan rate of 50 mVs^{-1} vs Ag/AgCl wire.

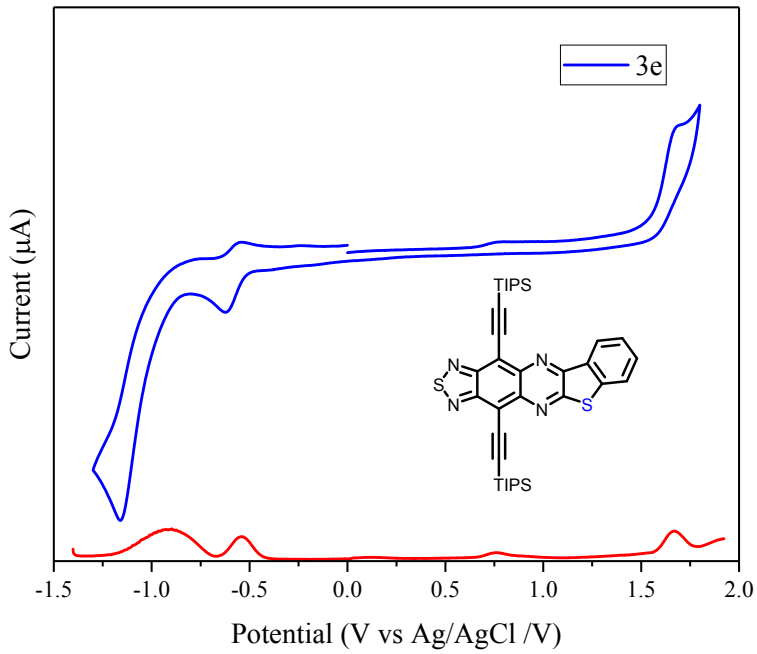

Figure S11. The DPV (red) and CV (blue) of **3e** in CH_2Cl_2 and 0.1 M Bu_4NPF_6 on a Pt electrode at a scan rate of 50 mVs^{-1} vs Ag/AgCl wire.

5. The mobility of typical products.

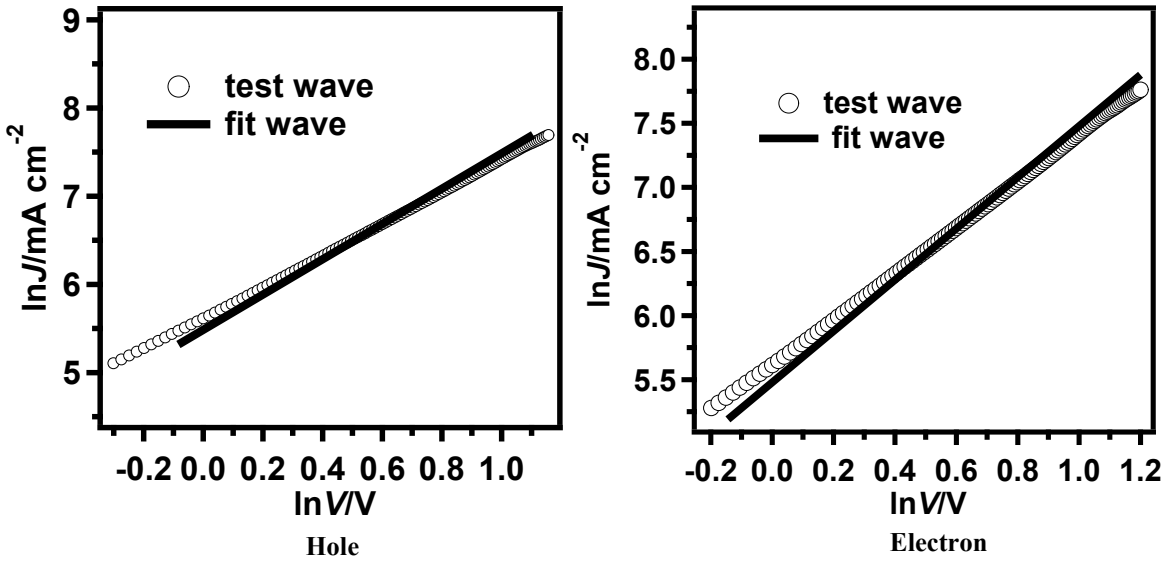

Figure S12. The ln*J*-ln*V* curve for **3c**

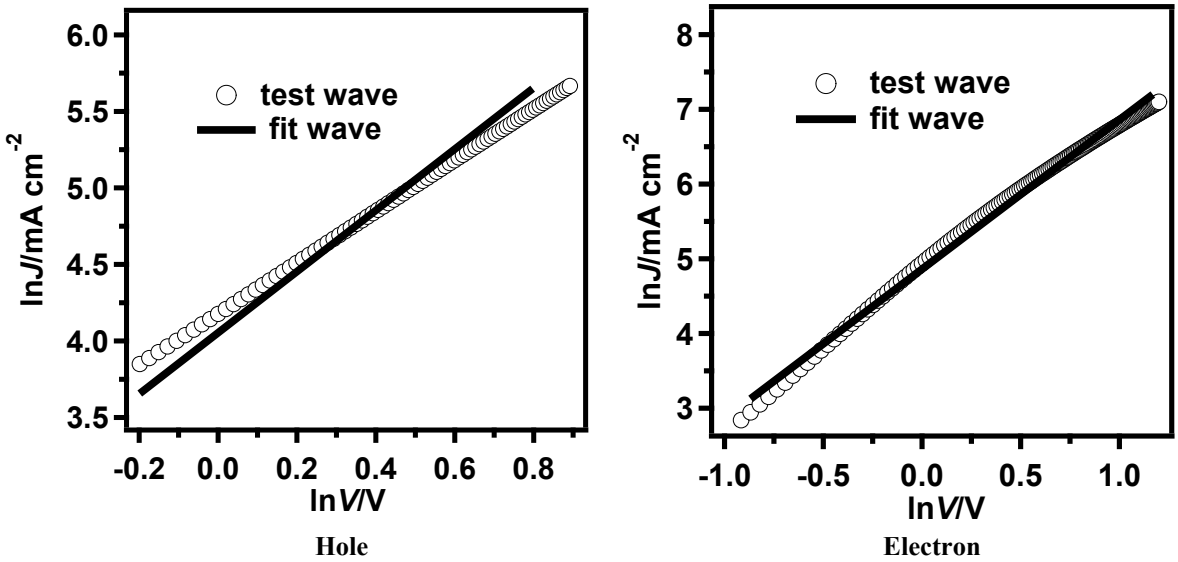

Figure S13. The ln*J*-ln*V* curve for **3d**

Table S1 the hole and electronic mobilities for **3c** and **3d**

Active layer	μ_h ($cm^2V^{-1}s^{-1}$)	μ_e ($cm^2V^{-1}s^{-1}$)
3c	$(2.77\pm0.04)\times10^{-4}$	$(2.81\pm0.07)\times10^{-4}$
3d	$(0.69\pm0.02)\times10^{-4}$	$(1.45\pm0.02)\times10^{-4}$

6. Single crystal structures

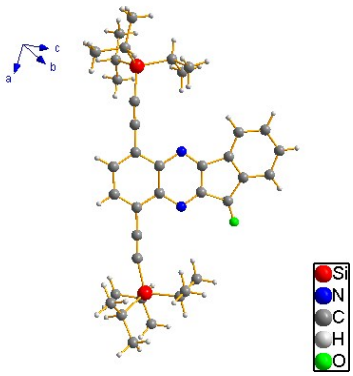

Compound	**3a** CCDC: 1951243
Empirical formula	$C_{37}H_{48}N_2OSi_2$
Formula weight	592.95
Temperature/K	173(2)
Crystal system	triclinic
Space group	P-1
a/Å	10.7016(9)
b/Å	12.9670(10)
c/Å	13.0146(10)
α/	79.414(2)
β/	72.908(2)
γ/	87.393(3)
Volume/Å^3	1696.8(2)
Z	2
μ/mm^{-1}	0.135
F(000)	640.0
Radiation	MoKα (λ = 0.71073)
2Θ range for data collection/	4.384 to 56.648
Index ranges	$-14 \leq h \leq 14$, $-17 \leq k \leq 17$, $-17 \leq l \leq 17$
Reflections collected	18939
Independent reflections	8376 [R_{int} = 0.0512, R_{sigma} = 0.0787]
Data/restraints/parameters	8376/0/379
Goodness-of-fit on F^2	1.037
Final R indexes [I>=2σ (I)]	R_1 = 0.0697, wR_2 = 0.1626
Final R indexes [all data]	R_1 = 0.1127, wR_2 = 0.1893
Largest diff. peak/hole / e Å^{-3}	0.78/-0.55

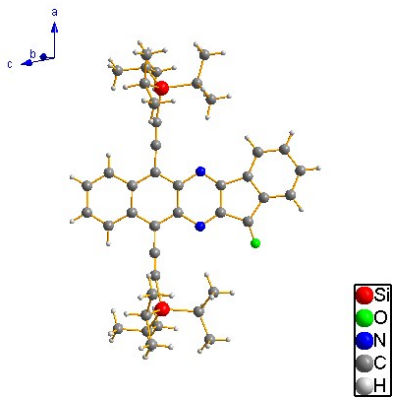

Compound	**3b** CCDC: 1951249
Empirical formula	$C_{41}H_{50}N_2OSi_2$
Formula weight	643.01
Temperature/K	180.00(10)
Crystal system	monoclinic
Space group	C2/c
a/Å	35.3121(18)
b/Å	7.9802(4)
c/Å	26.6542(12)
α/°	90
β/°	99.715(4)
γ/°	90
Volume/Å^3	7403.4(6)
Z	8
μ/mm^{-1}	1.114
F(000)	2768.0
Radiation	CuKα (λ = 1.54184)
2Θ range for data collection/°	6.728 to 142.402
Index ranges	$-43 \leq h \leq 40$, $-9 \leq k \leq 9$, $-31 \leq l \leq 32$
Reflections collected	25836
Independent reflections	7110 [R_{int} = 0.0479, R_{sigma} = 0.0350]
Data/restraints/parameters	7110/0/427
Goodness-of-fit on F^2	1.052
Final R indexes [I>=2σ (I)]	R_1 = 0.0439, wR_2 = 0.1178
Final R indexes [all data]	R_1 = 0.0479, wR_2 = 0.1211
Largest diff. peak/hole / e Å^{-3}	0.38/-0.47

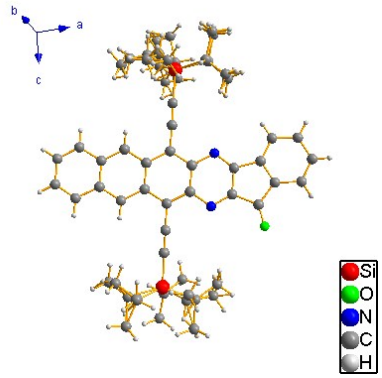

Compound	**3c** CCDC: 1951250
Empirical formula	$C_{45}H_{51}N_2OSi_2$
Formula weight	692.05
Temperature/K	297
Crystal system	triclinic
Space group	P-1
a/Å	8.2528(5)
b/Å	14.9237(12)
c/Å	17.2022(12)
α/°	87.976(6)
β/°	79.647(5)
γ/°	85.341(6)
Volume/Å^3	2076.8(3)
Z	2
μ/mm^{-1}	1.027
F(000)	742.0
Radiation	CuKα (λ = 1.54178)
2Θ range for data collection/°	5.942 to 141.466
Index ranges	$-9 \leq h \leq 7$, $-18 \leq k \leq 18$, $-20 \leq l \leq 18$
Reflections collected	15146
Independent reflections	7776 [R_{int} = 0.0188, R_{sigma} = 0.0321]
Data/restraints/parameters	7776/425/607
Goodness-of-fit on F^2	1.030
Final R indexes [I>=2σ (I)]	R_1 = 0.0736, wR_2 = 0.2164
Final R indexes [all data]	R_1 = 0.1068, wR_2 = 0.2625
Largest diff. peak/hole / e Å^{-3}	0.33/-0.25

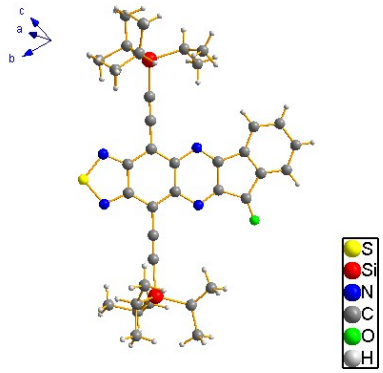

Compound	**3d** CCDC: 1951263
Empirical formula	$C_{37}H_{46}N_4OSSi_2$
Formula weight	651.03
Temperature/K	293(2)
Crystal system	triclinic
Space group	P-1
a/Å	8.0685(5)
b/Å	14.3842(11)
c/Å	18.1853(11)
α/°	67.428(6)
β/°	79.859(5)
γ/°	81.380(6)
Volume/Å^3	1910.6(2)
Z	2
μ/mm^{-1}	1.595
F(000)	604.0
Radiation	CuKα (λ = 1.54178)
2Θ range for data collection/°	6.682 to 141.408
Index ranges	$-9 \leq h \leq 7$, $-17 \leq k \leq 17$, $-21 \leq l \leq 21$
Reflections collected	14061
Independent reflections	7181 [R_{int} = 0.0220, R_{sigma} = 0.0308]
Data/restraints/parameters	7181/24/408
Goodness-of-fit on F^2	1.046
Final R indexes [I>=2σ (I)]	R_1 = 0.0743, wR_2 = 0.2295
Final R indexes [all data]	R_1 = 0.1019, wR_2 = 0.2712
Largest diff. peak/hole / e Å^{-3}	0.59/-0.36

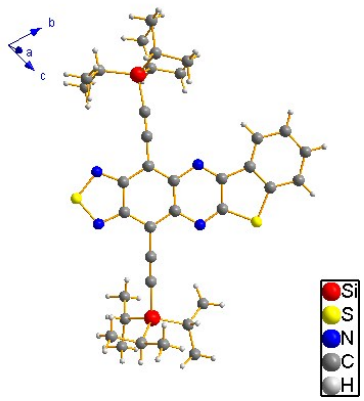

Compound	**3e** CCDC: 1951264
Empirical formula	$C_{36}H_{46}N_4S_2Si_2$
Formula weight	655.07
Temperature/K	293(2)
Crystal system	triclinic
Space group	P-1
a/Å	7.7604(9)
b/Å	14.5145(16)
c/Å	18.046(2)
α/°	69.651(11)
β/°	79.985(11)
γ/°	86.698(9)
Volume/Å^3	1876.7(4)
Z	2
μ/mm^{-1}	2.114
F(000)	700.0
Crystal size/mm^3	0.4 × 0.3 × 0.3
Radiation	CuKα (λ = 1.54178)
2Θ range for data collection/	6.826 to 152.72
Index ranges	$-9 \leq h \leq 9$, $-14 \leq k \leq 17$, $-22 \leq l \leq 21$
Reflections collected	13573
Independent reflections	7044 [R_{int} = 0.0347, R_{sigma} = 0.0533]
Data/restraints/parameters	7044/0/397
Goodness-of-fit on F^2	1.029
Final R indexes [I>=2σ (I)]	R_1 = 0.0845, wR_2 = 0.2516
Final R indexes [all data]	R_1 = 0.1303, wR_2 = 0.3184
Largest diff. peak/hole / e Å^{-3}	0.45/-0.34

7. NMR spectra

3a ^{1}H NMR (400 MHz) ^{13}C NMR (125 MHz) in $CDCl_3$, 298K

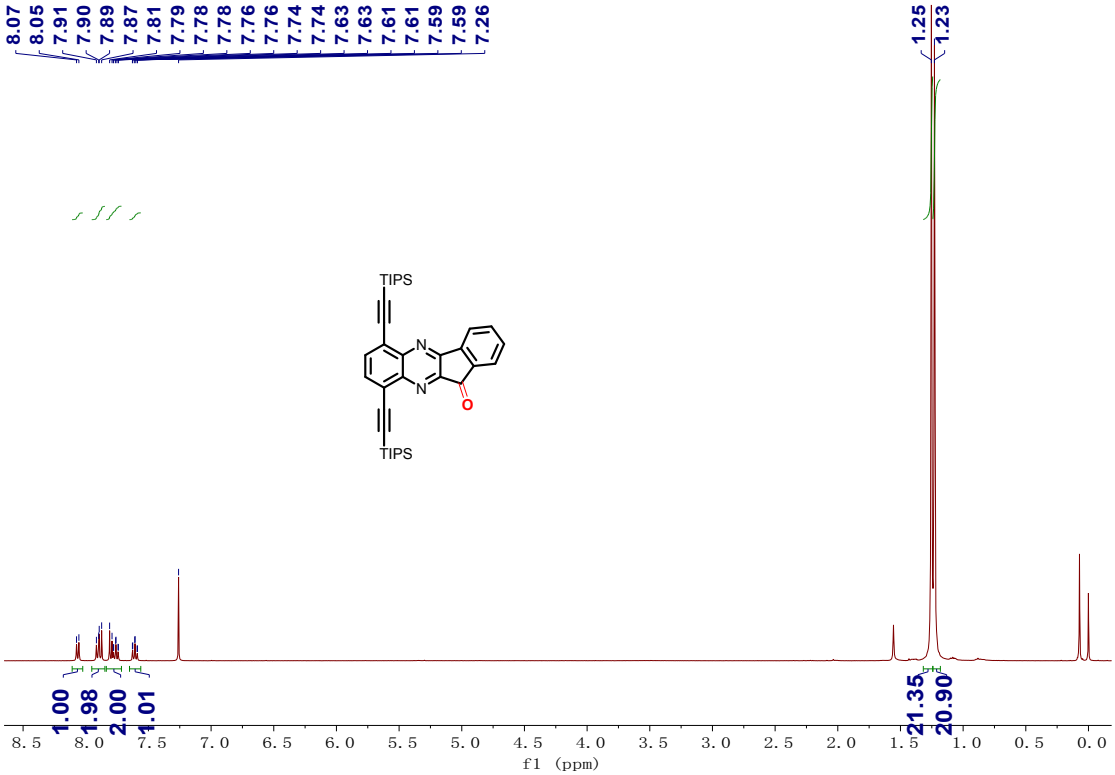

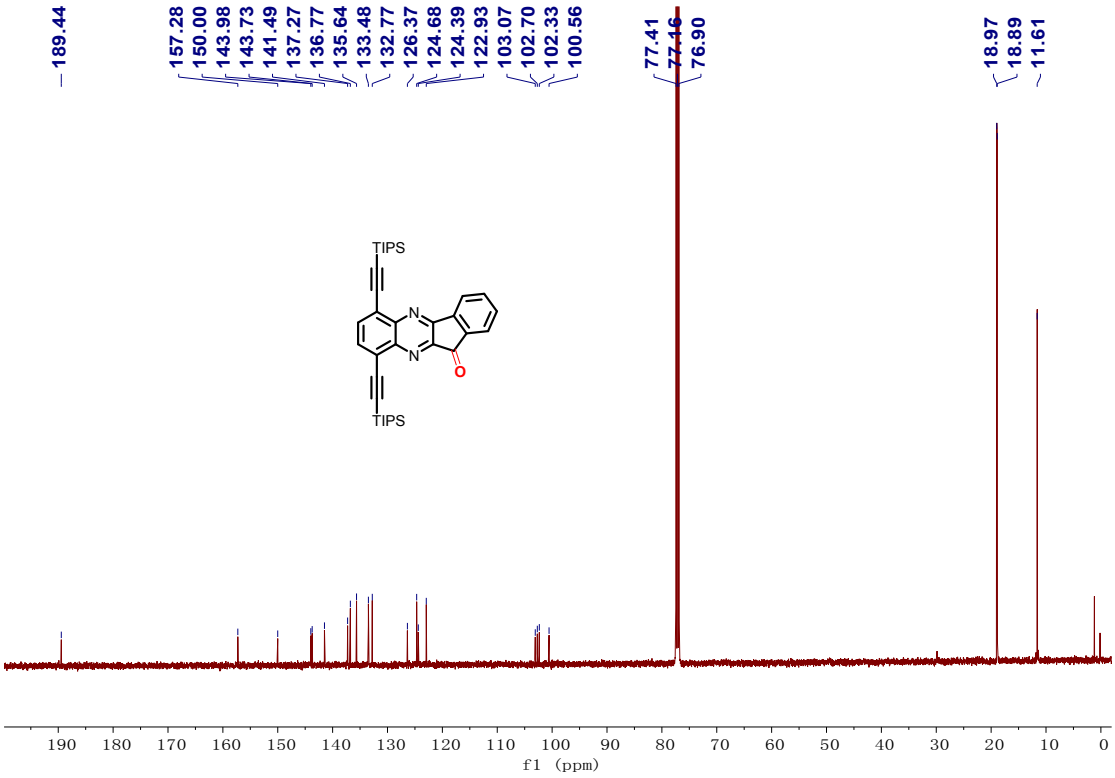

3b ^{1}H NMR (400 MHz) ^{13}C NMR (100 MHz) in $CDCl_3$, 298K

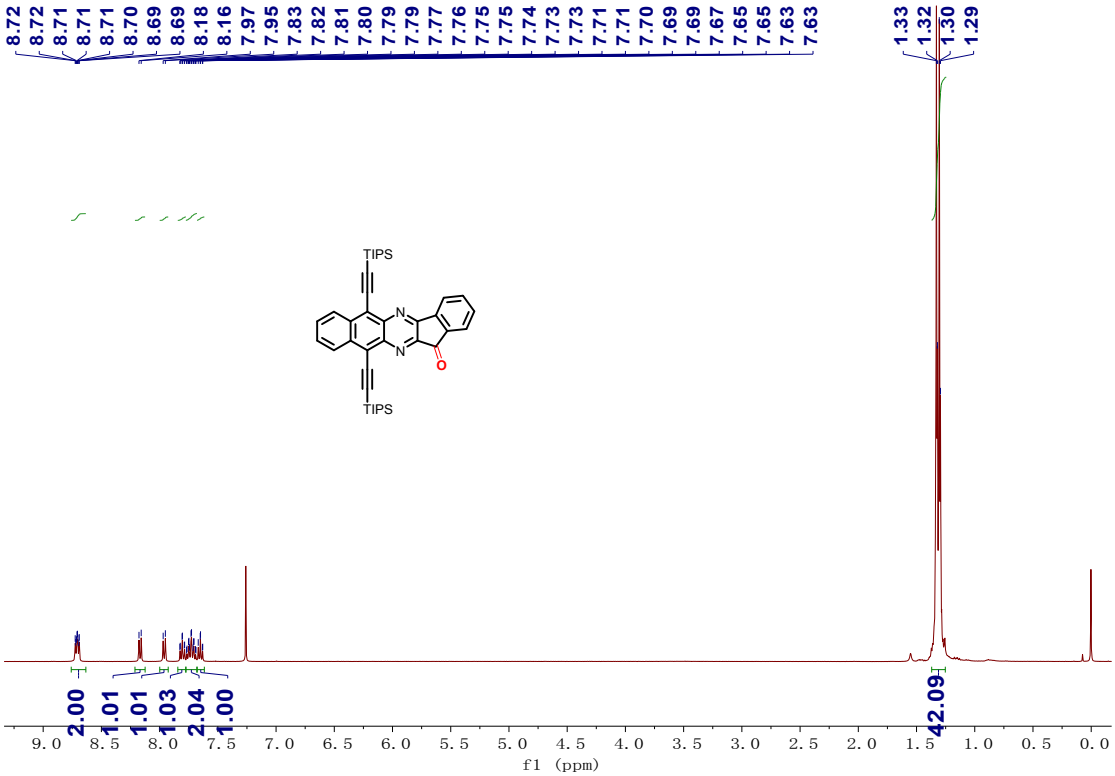

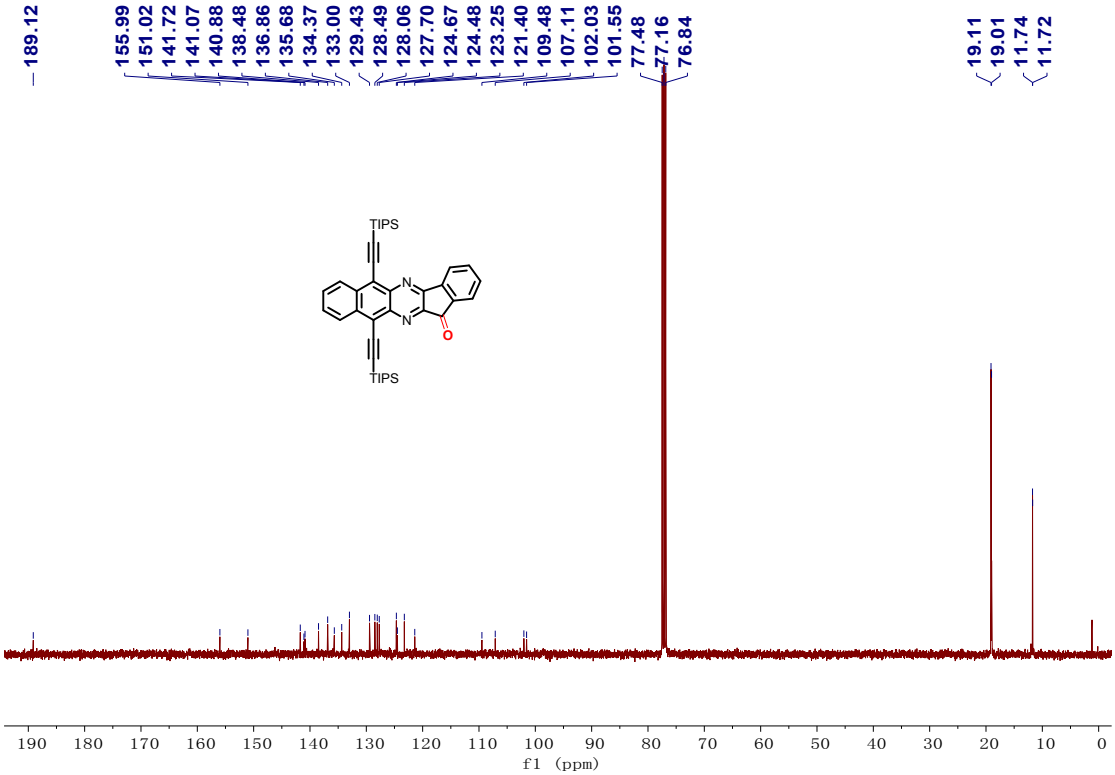

3c ^{1}H NMR (400 MHz) ^{13}C NMR (125 MHz) in $CDCl_3$, 298K

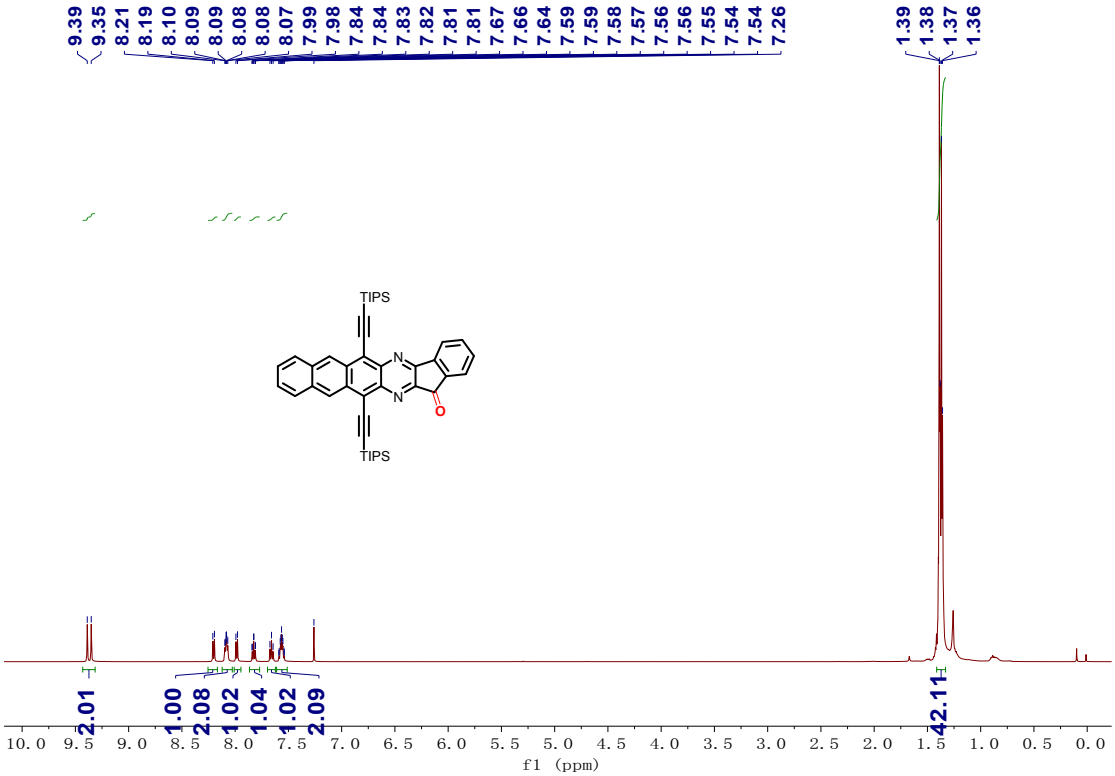

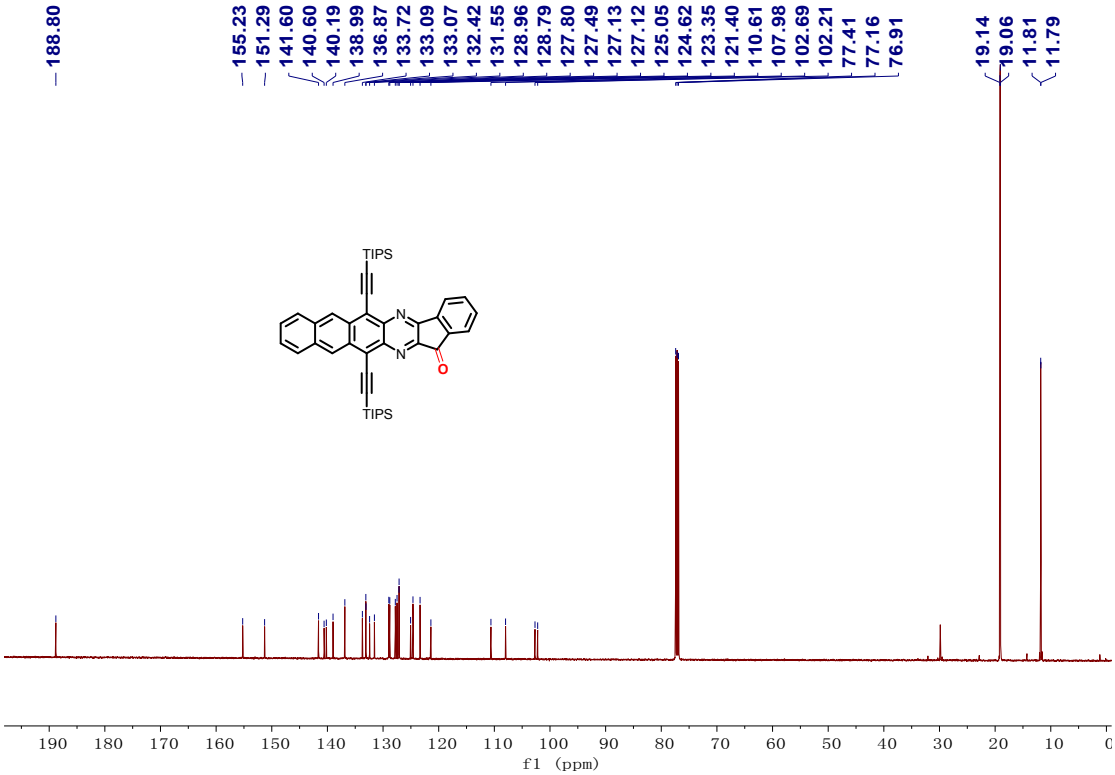

3d ^{1}H NMR (400 MHz) ^{13}C NMR (100 MHz) in $CDCl_3$, 298K

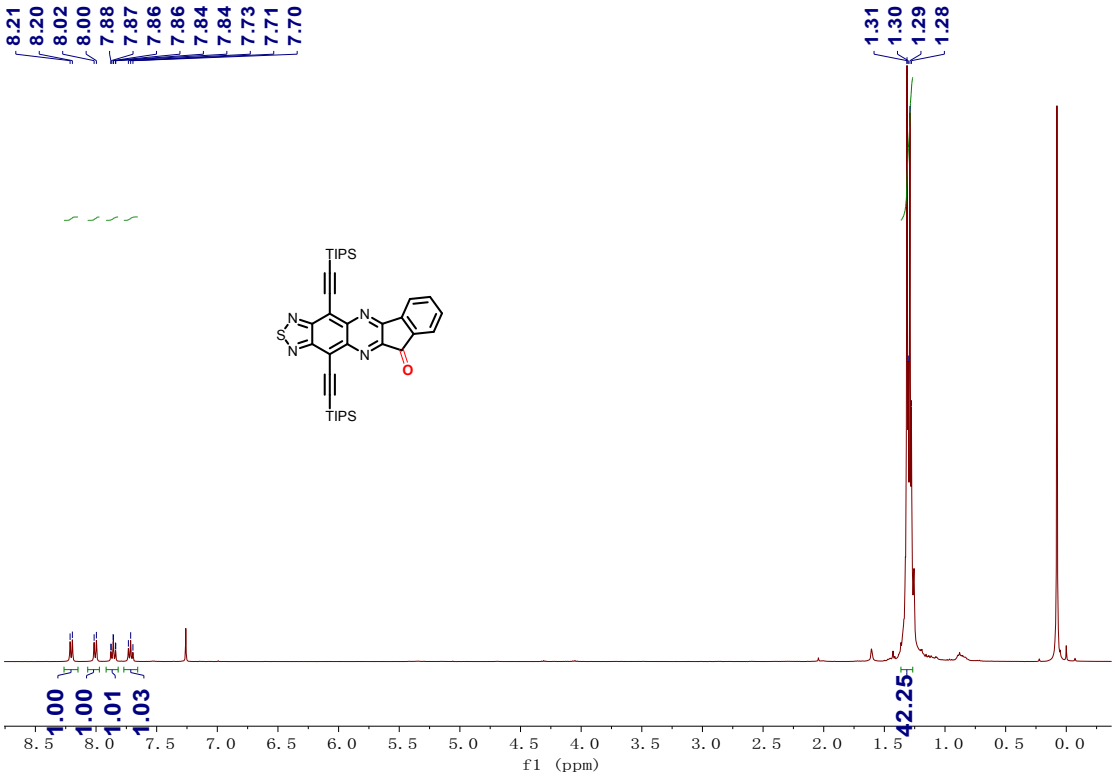

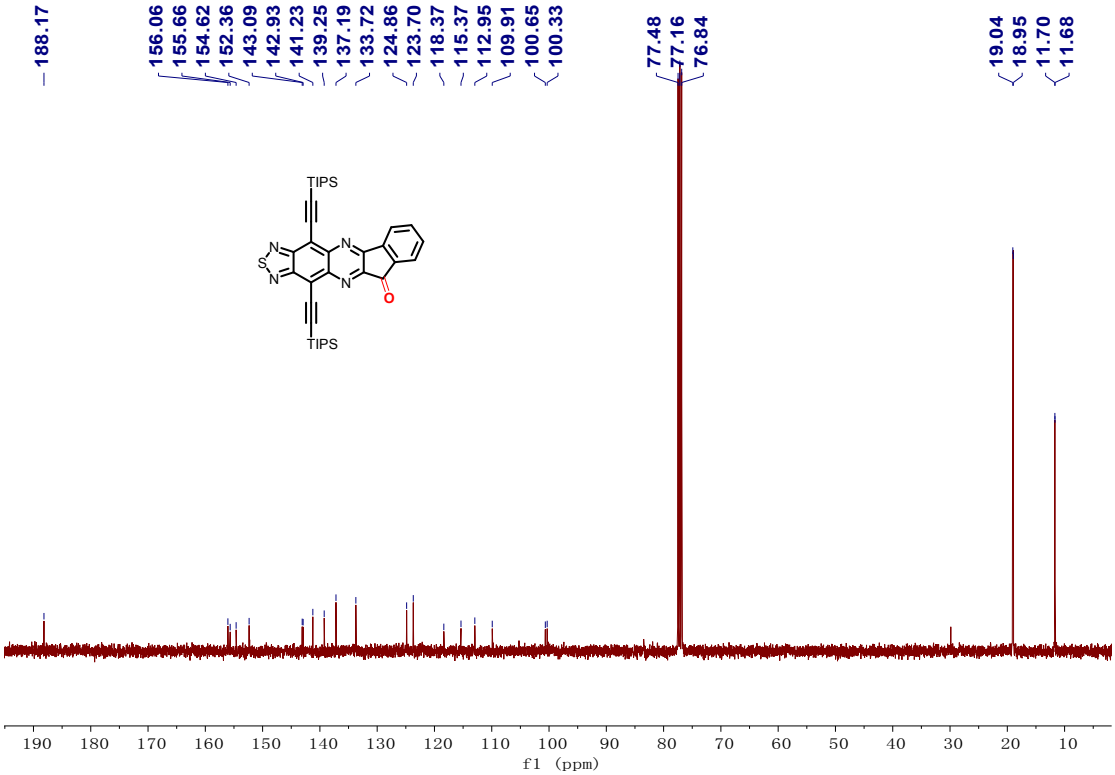

3e ^{1}H NMR (400 MHz) ^{13}C NMR (100 MHz) in $CDCl_3$, 298K

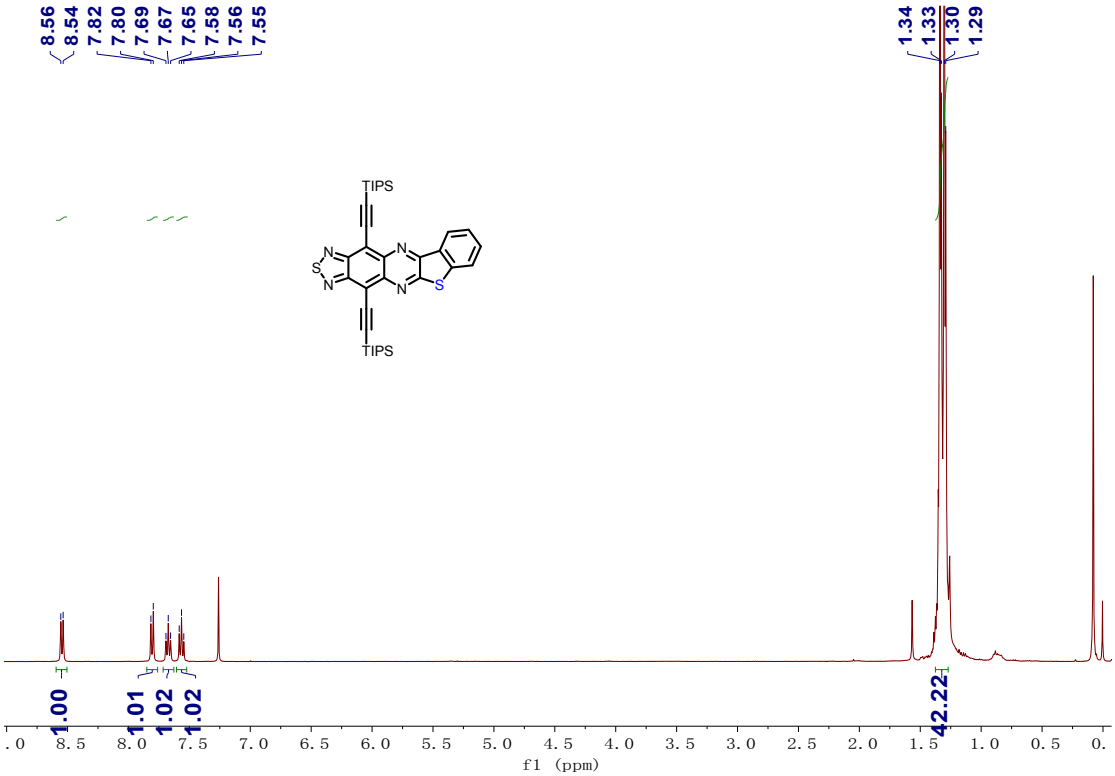

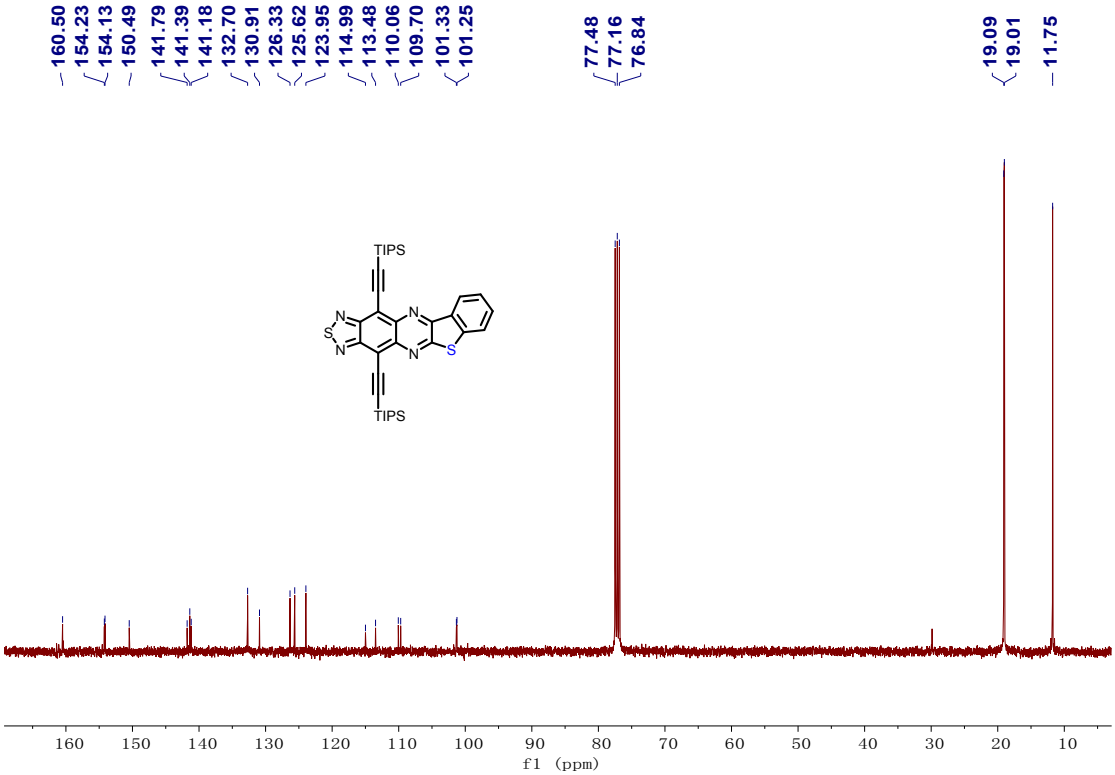

8. MALDI-TOF-MS spectra

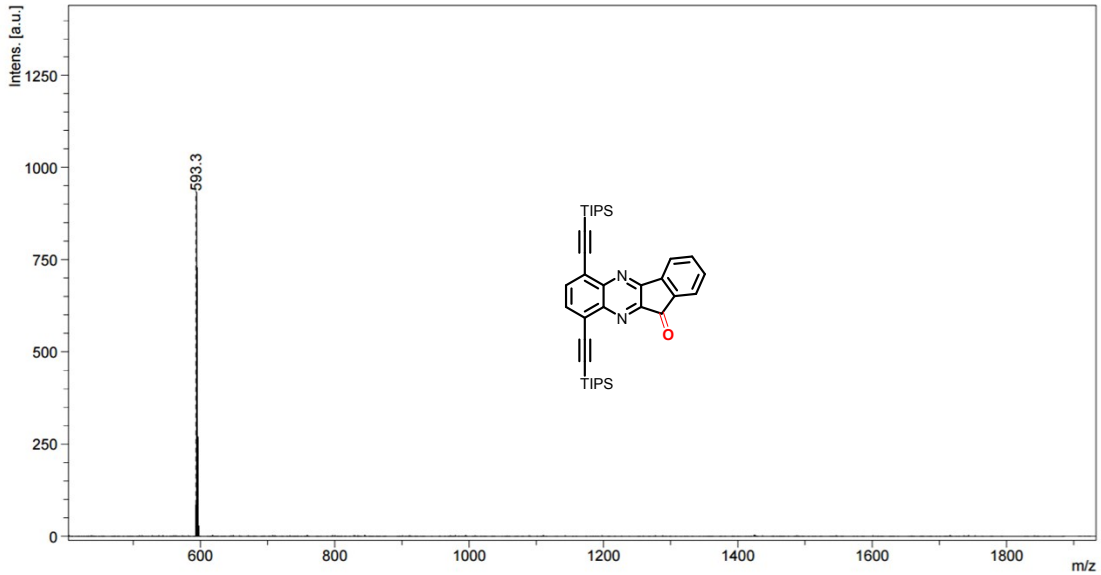

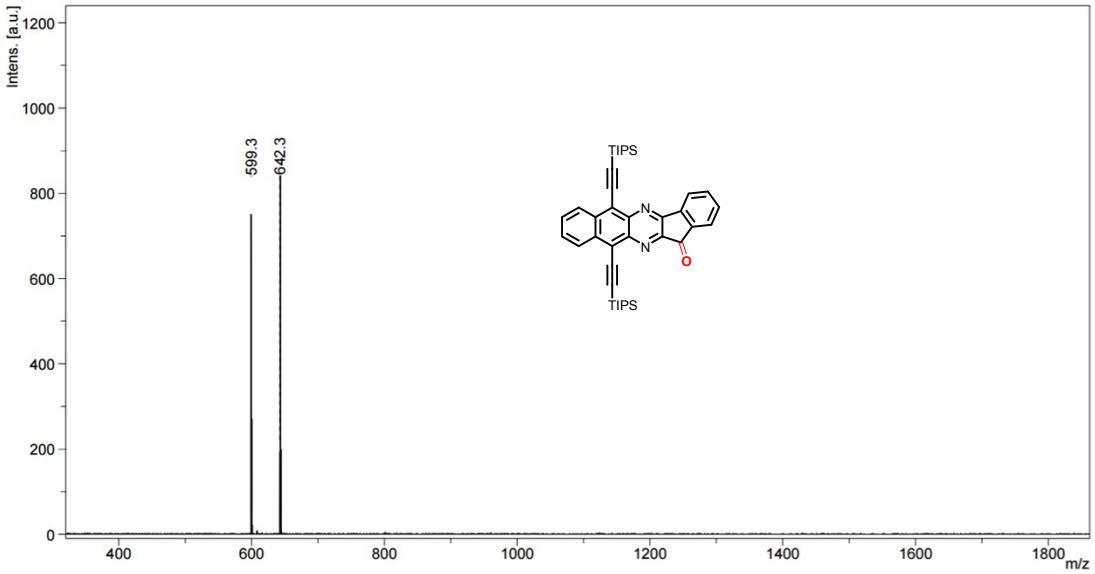

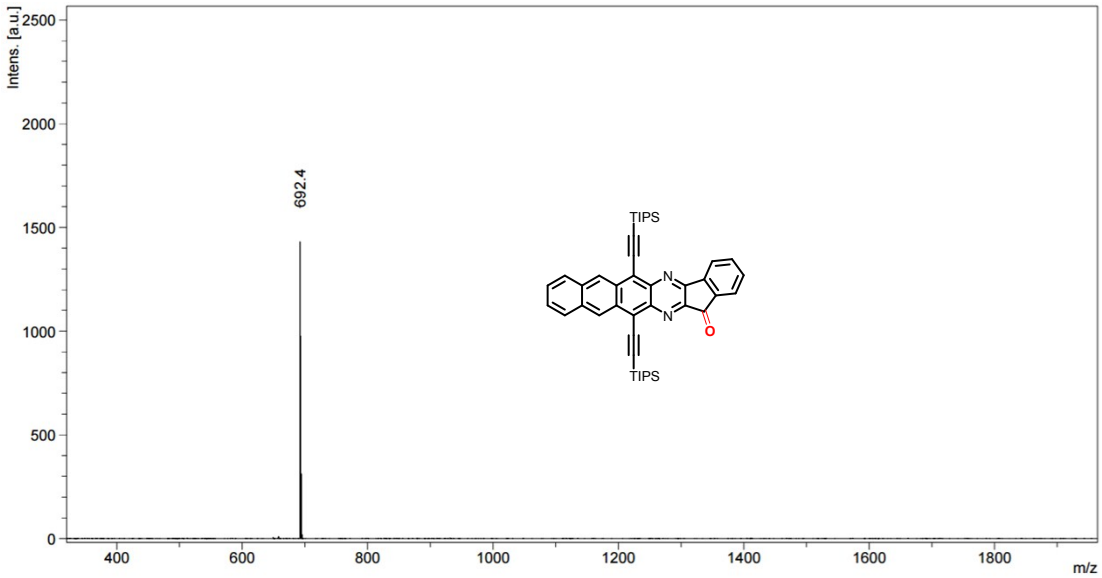
Intens. [a.u.]
692.4
TIPS
TIPS
m/z

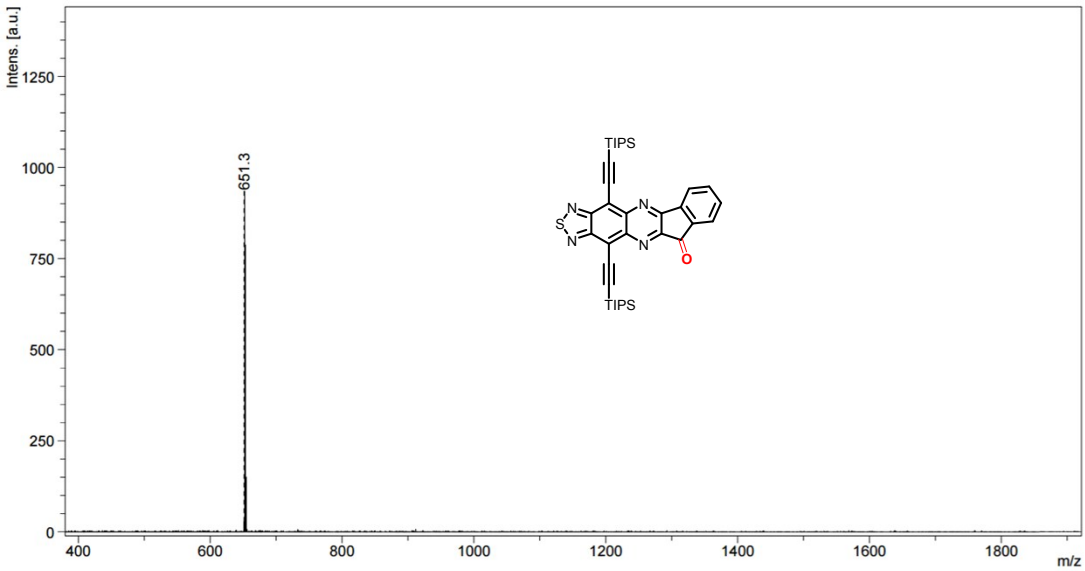
Intens. [a.u.]
651.3
TIPS
TIPS
m/z

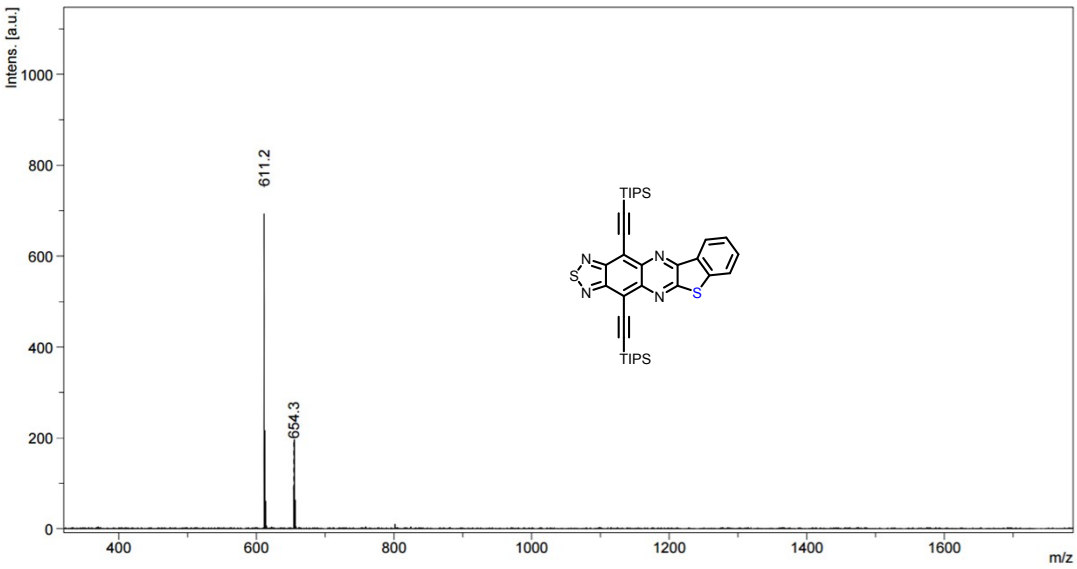
Intens. [a.u.]
611.2
654.3
TIPS
TIPS
m/z

9. IR spectra

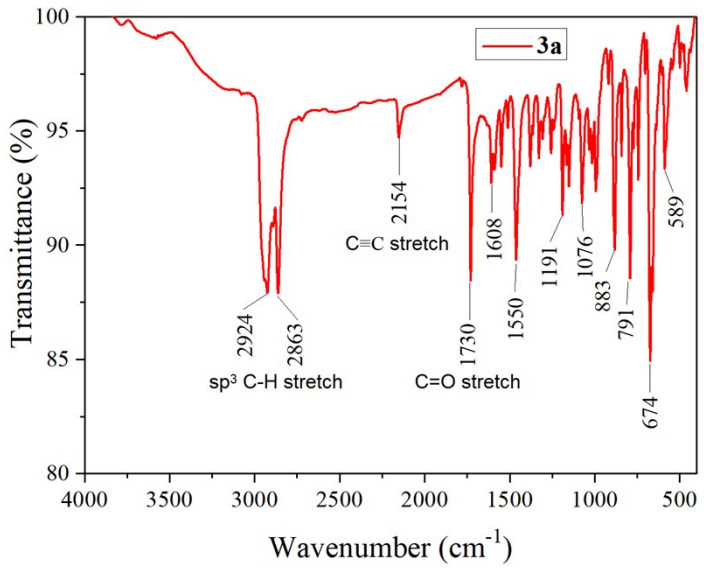

Figure S14. the IR spectra of **3a**

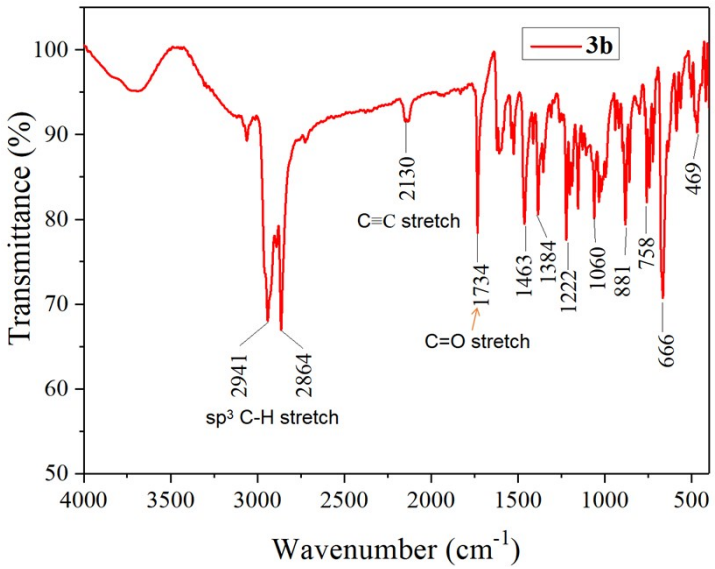

Figure S15. the IR spectra of **3b**

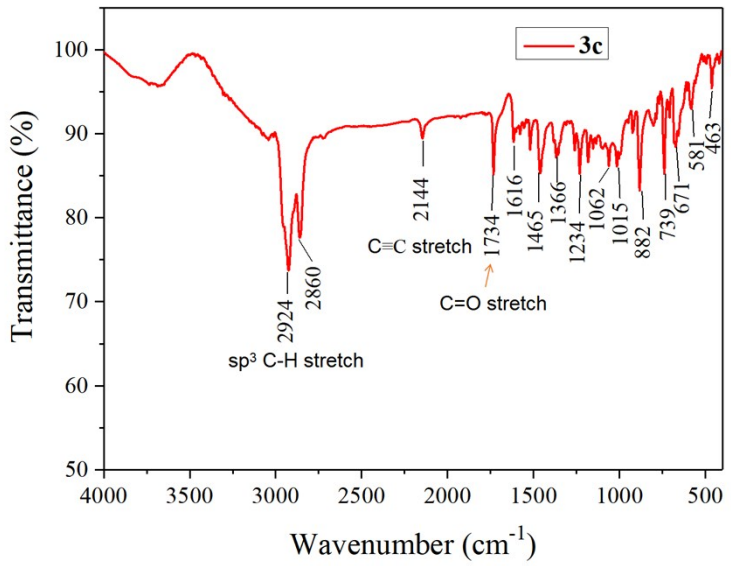

Figure S16. the IR spectra of **3c**

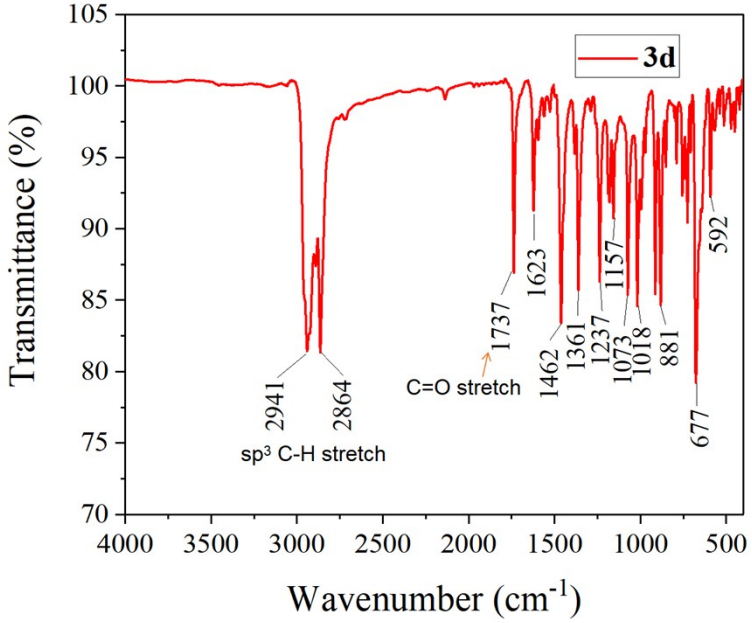

Figure S17. the IR spectra of **3d**

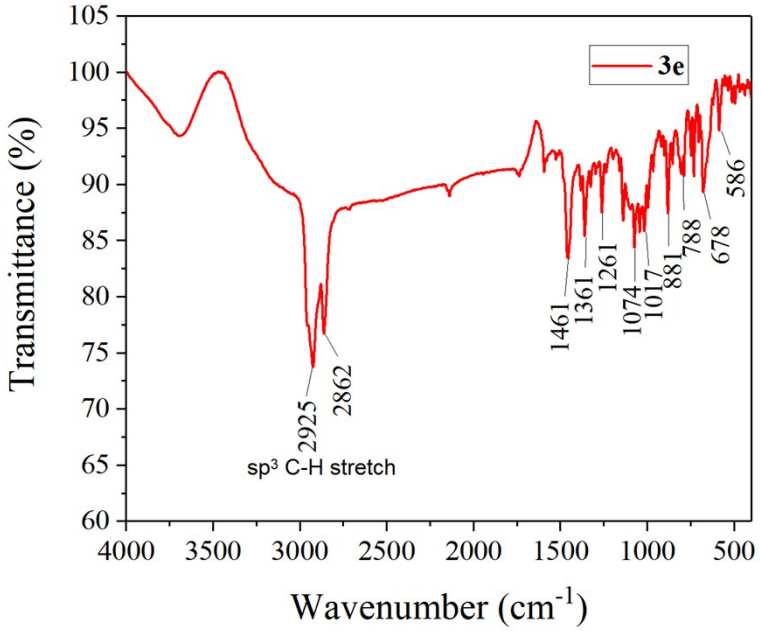

Figure S18. the IR spectra of **3e**

10. TGA data

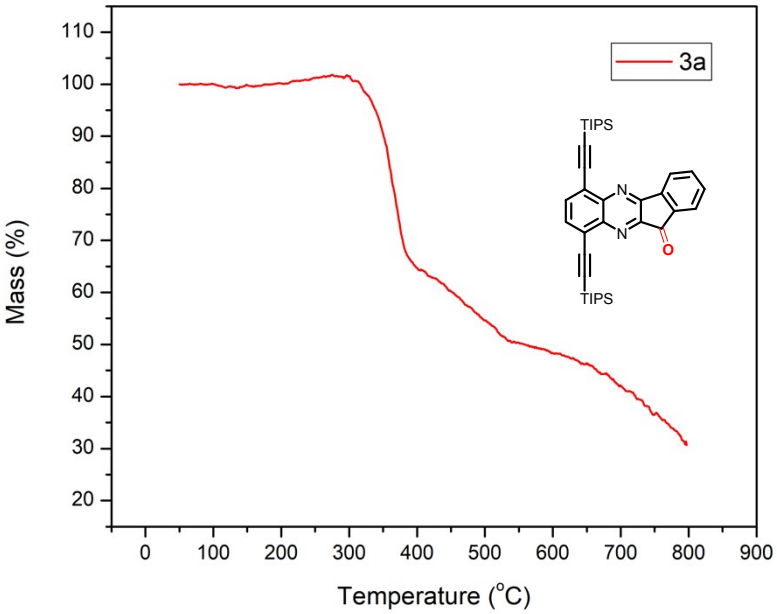

Figure S19. the TGA data of **3a**

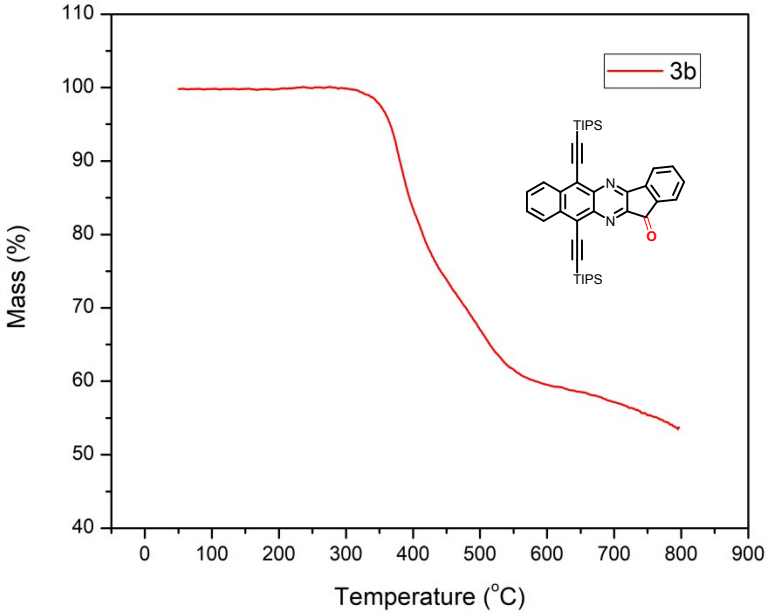

Figure S20. the TGA data of **3b**

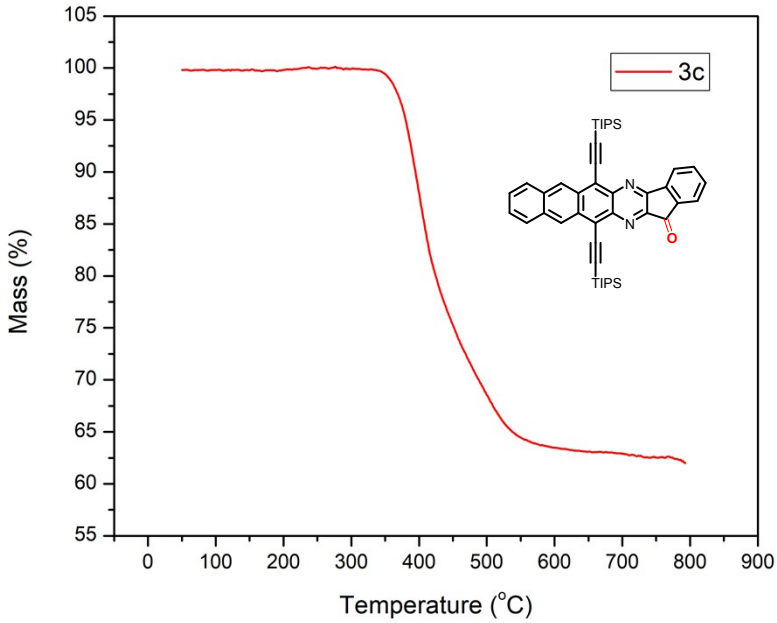

Figure S21. the TGA data of **3c**

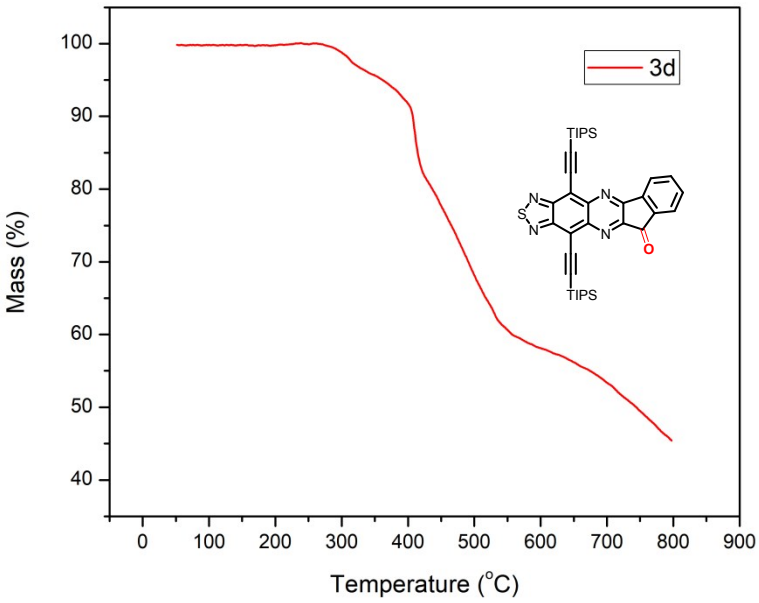

Figure S22. the TGA data of **3d**

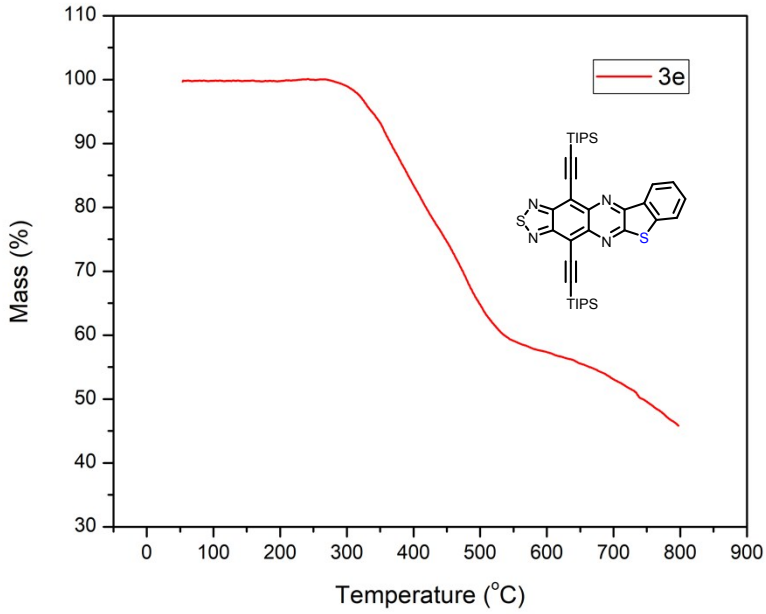

Figure S23. the TGA data of **3e**